Effects of noise on CSEM interferometry with synthetic aperture sources

Jürg Hunziker, Evert Slob and Kees Wapenaar, Delft University of Technology*
Yuanzhong Fan and Roel Snieder, Colorado School of Mines

SUMMARY

Interferometry by MDD for CSEM retrieves the subsurface reflection response which is free of any effects related to the medium above the receivers. Consequently, the problematic airwave as well as any other interaction of the signal with the air-water interface is removed. We apply interferometry by MDD in combination with the synthetic aperture source concept to overcome sampling problems. We investigate effects of random noise and receiver orientation and positioning errors using a numerical dataset. We have found that the method is robust against random noise because of the synthetic aperture source. Receiver orientation and positioning errors limit the bandwidth of the retrieved reflection response. Orientation errors are more severe than positioning errors.

INTRODUCTION

In frequency-domain marine Controlled Source Electromagnetics (CSEM), we create a low frequency (0.1 to 10 Hz), monochromatic signal with a source towed by a boat in the water. The resulting electromagnetic field diffuses on different paths to the receivers at the ocean bottom. The paths which contain the refracted or reflected signal of subsurface structures, such as a reservoir, are the interesting ones. But the signal can also travel directly from the source through the water to the receivers or, as the so called airwave, from the source along the air-water interface to the receivers. The direct field and the airwave dominate the data at small and large offsets, respectively. Since both signals do not contain any information about the subsurface, one aims to remove them from the data. For a description of the different travelpaths in CSEM see Amundsen et al. (2006), for an overview over CSEM see for example Constable (2010).

We propose to use interferometry by multidimensional deconvolution (MDD) to retrieve the reflection response, in other words the scattered subsurface Greens function. With interferometry by MDD, the medium above the receivers is replaced by a homogeneous halfspace with the same material parameters as just below the receivers. Consequently, the airwave and any other interactions of the signal with the air-water interface are removed. Furthermore, the direct field is removed and the sources are redatumed to the receiver locations (Wapenaar et al., 2008).

Since interferometry by MDD is a data driven method, it requires the data to be sampled properly. This means that the data need to be sampled at all offsets, including the area around zero offset, and also with a dense enough receiver spacing. Hunziker et al. (2010) showed that the spatial receiver sampling has to be smaller or equal than either the vertical distance between the source and the receivers or the length of the source antenna. It may not always be practical to tow the source vertically far away from the receivers (e.g. in a shallow sea) or to use a physically long source. To overcome the sampling problem, Hunziker et al. (2011) suggested to combine interferometry by MDD with the synthetic aperture source concept (Fan et al., 2010) in order to create a long source. With this approach, receiver sampling distances larger than 1200 m can be used. Consequently, the sampling problem of CSEM interferometry by MDD can be solved without changing the acquisition geometry.

In this paper, we investigate the effects of noise, positioning errors and orientation errors of the receivers on this method. Source positioning and orientation errors are not considered because the source is redatumed to the receivers without requiring knowledge about the source location or orientation.

METHOD

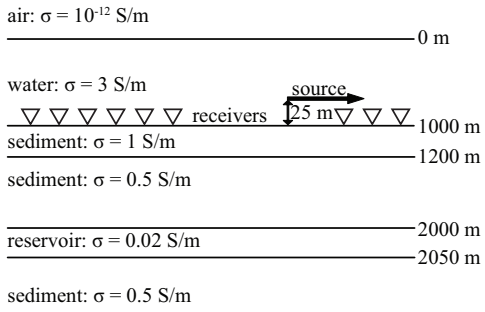

Figure 1: The configuration of the model (not to scale). The conductivity σ is given for each layer.

A dataset in 2D TM mode is modeled for a stack of layers, including a reservoir. The corresponding conductivity values σ are given in Figure 1. The receivers, indicated by triangles, are located at the ocean bottom. They record the inline electric, E_x, and the crossline magnetic, H_y, field components. The source, indicated in the figure by an arrow, is located 25 m above the receivers, has a physical length of 80 m and emits the source signal at a frequency of 0.5 Hz.

The electric field due to one source location is plotted in Figure 2a as a function of offset from the source location. Around zero offset, the horizontal field gradient is very steep what translates to large amplitudes at high wavenumbers in the wavenumber domain. In order to damp the signal at these high wavenumbers, a synthetic aperture source is created by summing the electromagnetic field over a range of 5000 m. Thereby, each field is weighted following a Gaussian distribution function

$$f(x) = \frac{1}{\sqrt{2\pi\gamma^2}} \exp\left(-\frac{(x-x_0)^2}{2\gamma^2}\right), \qquad (1)$$

where x_0 is the center of the synthetic aperture source. The parameter γ is chosen to be one eighth of the length of the synthetic aperture source. The parameter x represents the source location in inline direction. The resulting electric field due to a 5000 m long synthetic aperture source is plotted in Figure 2b. The resulting curve is much smoother and can therefore be sampled sparser. The same procedure is also applied to the crossline magnetic field component.

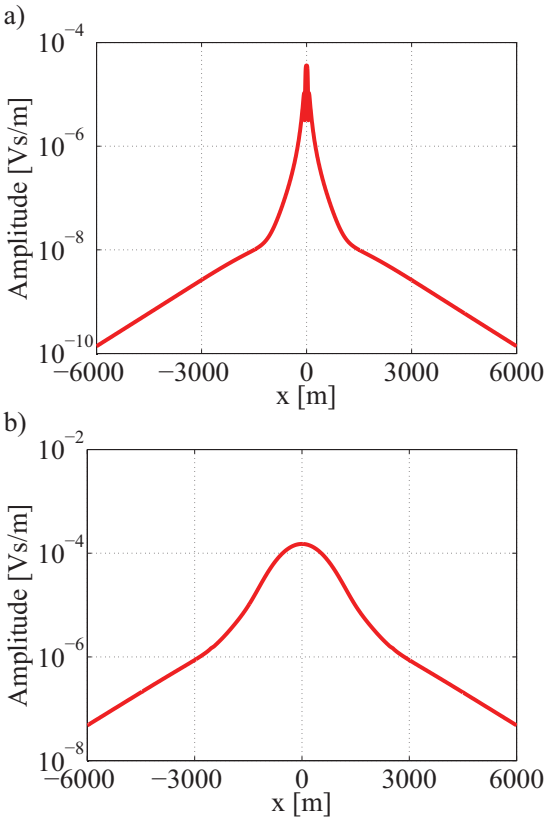

Figure 2: a) The electric field as a function of offset for one source position of an 80 m long source. b) The electric field due to a synthetic aperture source of a length of 5000 m.

The electromagnetic fields due to this synthetic aperture source are decomposed into upward and downward decaying components $\hat{\mathbf{P}}^-$ and $\hat{\mathbf{P}}^+$, respectively, using an algorithm by Slob (2009). Written in matrix notation (Berkhout, 1982), these two components can be related to each other through the reflection response $\hat{\mathbf{R}}_0^+$

$$\hat{\mathbf{P}}^- = \hat{\mathbf{R}}_0^+ \hat{\mathbf{P}}^+, \tag{2}$$

where the circumflex indicates the space-frequency domain. Each column of the matrices contains various receiver positions for a fixed source position, while for the rows the situation is reversed. The superscript $^+$ of $\hat{\mathbf{R}}_0^+$ indicates that this reflection response originates in a downward decaying field. The subscript $_0$ represents the absence of heterogeneities above the receiver level.

In the last step, we solve equation 2 for the reflection response $\hat{\mathbf{R}}_0^+$. This can for example be done through a least-squares inversion

$$\hat{\mathbf{R}}_0^+ = \hat{\mathbf{P}}^- \left(\hat{\mathbf{P}}^+\right)^\dagger \left[\hat{\mathbf{P}}^+ \left(\hat{\mathbf{P}}^+\right)^\dagger + \varepsilon^2 \mathbf{I}\right]^{-1}. \tag{3}$$

The superscript † denotes complex-conjugation and transposition and $\mathbf{I}$ is the identity matrix. The reflection response $\hat{\mathbf{R}}_0^+$ is basically the cross correlation of the upward decaying field with the downward decaying field $\hat{\mathbf{P}}^-(\hat{\mathbf{P}}^+)^\dagger$ deconvolved with the cross correlation of the downward decaying field with itself $\hat{\mathbf{P}}^+(\hat{\mathbf{P}}^+)^\dagger$. The stabilization parameter ε^2 prevents instabilities in the deconvolution process. If ε is chosen very large, the term $\varepsilon^2\mathbf{I}$ is much larger than $\hat{\mathbf{P}}^+(\hat{\mathbf{P}}^+)^\dagger$ and equation 3 is basically reduced to a scaled cross correlation. If ε is chosen too small, the inversion gets unstable. Consequently, a range of values for the stabilization parameter need to be tested in order to retrieve the reflection response well.

RESULTS

We applied interferometry by MDD to a numerical dataset which consists of 64 receiver stations with a sampling distance of 320 m. Interferometry by MDD works also for larger receiver sampling distances (Hunziker et al., 2011) but we have chosen this receiver sampling distance because noise effects are better visible on a relatively densely sampled curve.

The reflection response retrieved with equation 3 for a noise-free dataset is shown in the wavenumber domain and in the space domain in Figures 3a and 3b, respectively. The gray curve is a directly modeled reflection response. In other words, the gray curve is what we aim to retrieve from the electromagnetic fields by applying interferometry by MDD. The dashed red curve is the reflection response that we actually retrieve from the data. The reflection response is retrieved well within a limited bandwidth as can be seen from the wavenumber domain plot (Figure 3a). The length of this bandwidth depends on the receiver sampling distance. In the space domain (Figure 3b), some artifacts are present around an offset of 1500 m. These and other artifacts at larger offsets increase in amplitude if the stabilization parameter ε is decreased. The amplitude of the peak at zero offset depends in the same way strongly from the stabilization parameter.

We contaminated the data with random noise at a level of 10^{-11} Vs/m for the electric field and with a level of 10^{-8} As/m for the magnetic field. If we normalize these noise levels with the source dipole moment, i.e. the length of the source times the electric current of the source, we get noise levels of 10^{-13} Vs/(Am^2) and 10^{-10} As/(Am^2) for the electric and the magnetic field, respectively. These noise levels are two orders of magnitude larger than noise levels of current receivers (Constable, 2010). The retrieved reflection response from this dataset is shown in Figures 3c and 3d in the wavenumber domain and in the space domain, respectively. A comparison with the noise-free plots reveals that our method is hardly affected by these noise levels. This is due to the synthetic aperture source which averages out the noise by addition.

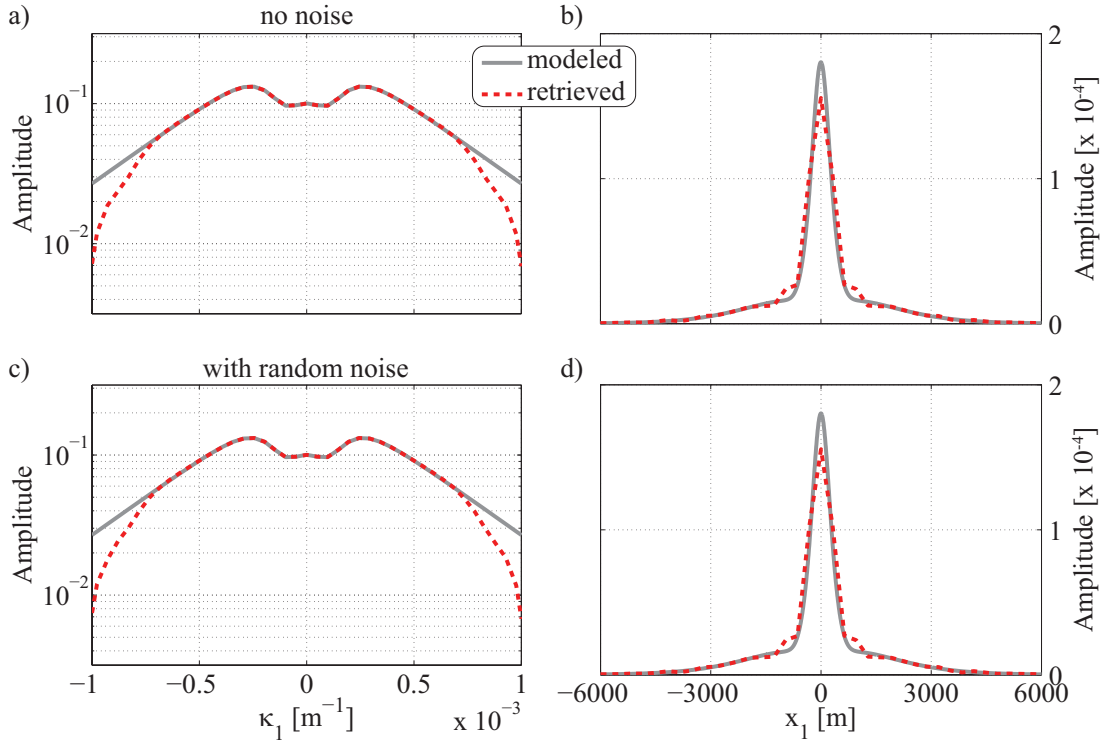

Figure 3: Retrieved reflection response (dashed red) for a dataset with 64 receivers separated by 320 m and directly modeled reflection response (solid gray). Left column shows the reflection response in the wavenumber domain and the right column in the space domain; a), b): without noise; c), d) with random noise added.

Besides random noise, errors in the receiver orientation and position information can disturb the data. In contrast, source orientation and position information errors do not harm interferometry by MDD because the method does not require any knowledge about the source. Therefore we do not consider source uncertainties.

We simulated random orientation errors of up to 10 degrees for the antennas measuring the electric field. The reflection response retrieved from that dataset is shown in Figures 4a and 4b. Comparing the wavenumber domain plot of the dataset with the orientation errors (Figure 4a) with the one of the noise-free dataset (Figure 3a) reveals that orientation errors strongly limit the bandwidth within which the reflection response is retrieved properly. In the space domain (Figure 4b), this leads to instabilities at intermediate and large offsets which can be damped with an increase in stabilization. This in turn leads to a more severe underestimation of the amplitude at zero offset.

We also simulated random positioning errors of up to $\pm$ 50 m. These rather large positioning errors were chosen because the method turned out to be hardly affected by smaller positioning errors. The retrieved reflection response is shown in Figures 4c and 4d. The effect of these positioning errors limits the bandwidth of the properly retrieved reflection response in a similar way as orientation errors. Under normal circumstances, positioning errors are much smaller and, therefore, have much less effect on the retrieved reflection response.

Finally, we combined orientation and positioning errors. The corresponding reflection response is shown in Figures 4e and 4f. The two kinds of errors add up, resulting in a further decreased band of wavenumbers which is retrieved properly.

CONCLUSIONS

We have applied the synthetic aperture source concept to avoid sampling problems and interferometry by MDD with the goal to remove the airwave and the direct field from CSEM data. This combination proves to be very robust against random noise, because the electromagnetic fields are stacked over a range of source positions in order to create a synthetically long source. Receiver orientation and positioning errors lead to a limited bandwidth within which the reflection response can be retrieved properly. Receiver orientation errors affect the data more than receiver positioning errors. For the interferometry method, source orientation and position are not relevant. Therefore, errors on the source side are ignored.

ACKNOWLEDGMENTS

This research is supported by the Dutch Technology Foundation STW, applied science division of NWO and the Technology Program of the Ministry of Economic Affairs (grant DCB.7913).

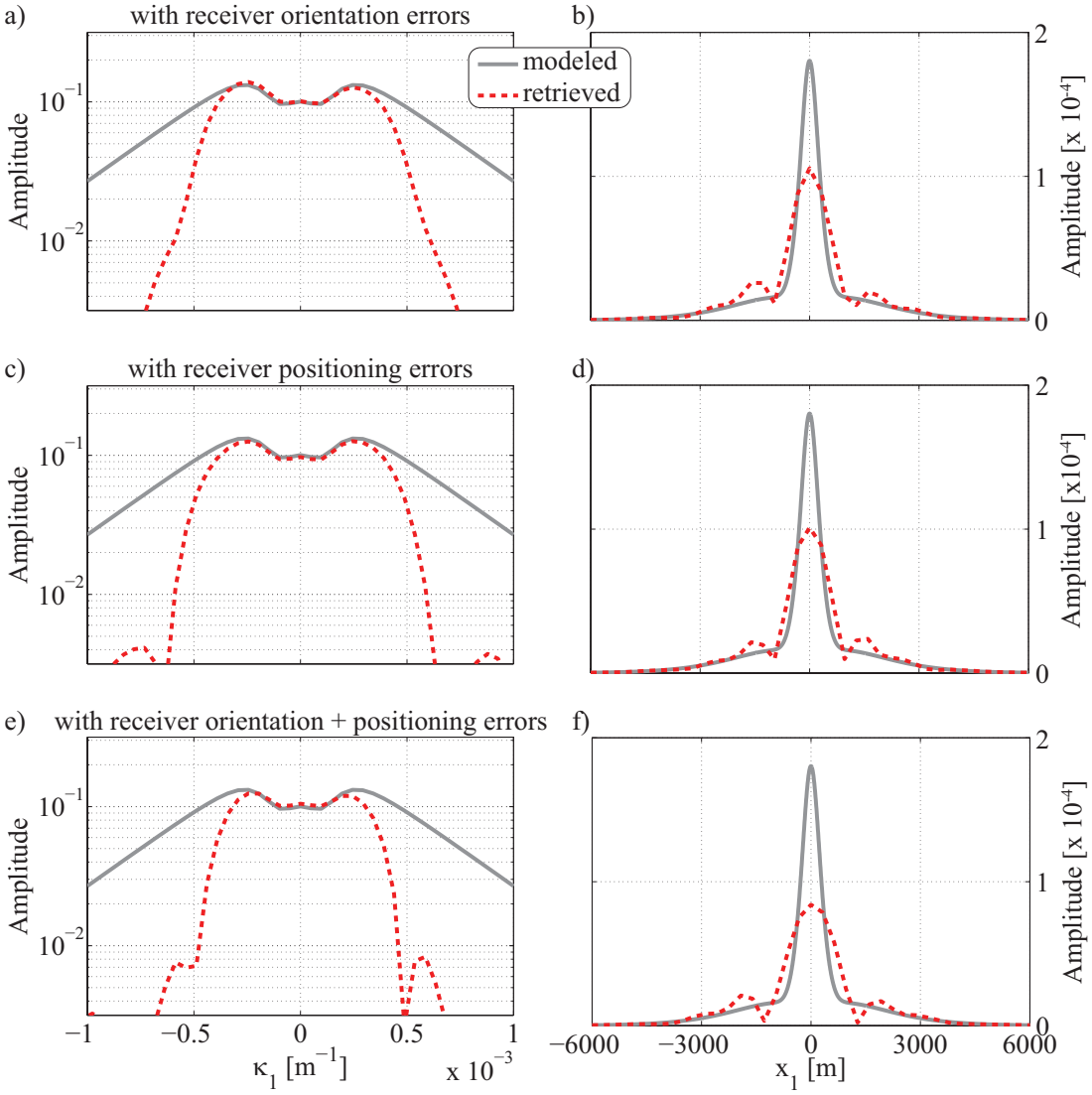

Figure 4: Retrieved reflection response as in Figure 3, but with a), b) orientation errors, c), d) positioning errors and e), f) orientation and positioning errors.

REFERENCES

Amundsen, L., L. Løseth, R. Mittet, S. Ellingsrud, and B. Ursin, 2006, Decomposition of electromagnetic fields into upgoing and downgoing components: Geophysics, **71**, G211–G223.

Berkhout, A. J., 1982, Seismic Migration. Imaging of Acoustic Energy by Wave Field Extrapolation: Elsevier.

Constable, S., 2010, Ten years of marine CSEM for hydrocarbon exploration: Geophysics, **75**, 75A67–75A81.

Fan, Y., R. Snieder, E. Slob, J. Hunziker, J. Singer, J. Sheiman, and M. Rosenquist, 2010, Synthetic aperture controlled source electromagnetics: Geophys. Res. Lett., **37**, L13305.

Hunziker, J., Y. Fan, E. C. Slob, K. Wapenaar, and R. Snieder, 2010, Solving spatial sampling problems in 2D-CSEM interferometry using elongated sources: 72nd EAGE Conference and Exhibition, Barcelona, Spain.

———, 2011, CSEM-interferometry using a synthetic aperture source: 73rd EAGE Conference and Exhibition, Vienna, Austria.

Slob, E., 2009, Interferometry by Deconvolution of Multicomponent Multioffset GPR Data: IEEE Transactions on Geoscience and Remote Sensing, **47**, 828–838.

Wapenaar, K., E. Slob, and R. Snieder, 2008, Seismic and electromagnetic controlled-source interferometry in dissipative media: Geophysical Prospecting, **56**, 419–434.